PHY 982 Homework 3

John Ash, Mengzhi Chen, Tong Li, Jason Surbrook

March 22, 2018

1 Choice of beam energies and potentials

The ^{12}C(d, p)^{13}C reaction is discussed in this work. The Coulomb barrier between ^{12}C and deutron is about 2.03 MeV. Then, two deuteron beam energies are studied, one is 2.84 MeV near the Coulomb barrier; another one is 4.51 MeV which is about 2 times higher than the barrier .

At both of the experimental energies chosen, the reaction is more accurately modeled as a compound reaction, as mentioned in [1]. Therefore our calculations using FRESCO may not yield satisfying agreement with experiment.

Optical potentials are needed that described the incoming and outgoing distorted waves. These are interactions between: ^{12}C, d [2] and ^{12}C, p[3]. For the deuteron wave-function, the binding for the proton and neutron was described by a simple gaussian potential

$$V_{np}(r) = -72.15e^{-(r/1.484)^2}. \tag{1}$$

scaled to reproduce a bound state at 2.2 MeV.

The neutron that is transferred in the reaction is expected to occupy a $1p_{1/2}$ orbit with an experimental single-particle binding energy of 4.946 MeV. The FRESCO calculation dynamically adjusts the Woods-Saxon depth for ^{13}C to reproduce this energy.

2 Results of DWBA post-form calculations

In a transfer reaction A(d,p)B showed in Fig. 1, by introduction the auxiliary potential $U_f(R_2)$, the transfer T-matrix has a formula [4]

$$T_{post} = \langle \phi_{nA}\chi^{(-)}_{pB} \left| V_{np}(r_1) + U_{pA}(r_p) - U_f(R_2) \right| \Psi^{(+)}_1(\vec{r}_1, \vec{R}_1) \rangle, \tag{2}$$

where ϕ_{nA} and χ_{pB} are bound states wave-functions. Under first-order DWBA, it becomes

$$T^{DWBA}_{post} = \langle \phi_{nA}\chi^{(-)}_{pB} \left| V_{np}(r_1) + U_{pA}(r_p) - U_f(R_2) \right| \phi_{np}\chi_{dA} \rangle. \tag{3}$$

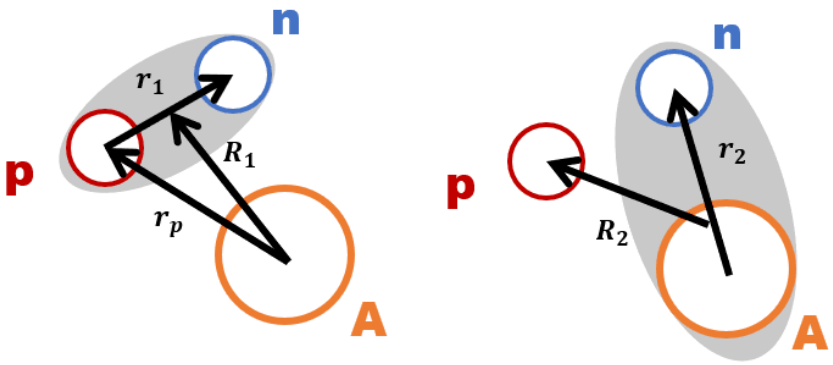

Figure 1: Coordinates used in one neutron transfer reaction.

Besides that, we still need information for the auxiliary potential $U_f(R_2)$. It's usually chosen as $U_{pB}(R_2)$ fitted from elastic scattering. We name $V_{np}(r_1)$ as binding potential and the rest two remnants.

Here are three different handling methods we used in our calculations.

1. Zero range (ZR) approximation: Remnants are neglected; $V_{np}(r_1)$ is considered as a local interaction with strength D_0. Correspondingly, the T-matrix becomes

$$T_{post}^{ZR-DWBA} = D_0 \langle \phi_{nA}(R_1) \chi_{pB}^{(-)} | \chi_{dA}(R_1) \rangle. \tag{4}$$

   It now relies on R_1 only, which simplifies calculation.

2. First-order DWBA, finite-range interactions, without or with full complex remnant: The former abandons the remnants but the latter keeps, as well as the nonlocality of $V_{np}(r_1)$ is preserved in both.

Our results are generated with radius $r_{match} = 60$ fm, partial waves up to $j_{max} = 55$ (in units of $\hbar$) and step size $rintp = 0.2$ fm. To test the convergence, these values are modified up to $r_{match} = 80$ and $j_{max} = 70$ and down to $rintp = 0.01$ for the full complex remnant cases. The differential cross sections deviate $< 2\%$ between calculation initializations. Furthermore, as long as $rintp > 0.05$, the deviation from primary initializations is $< 0.5\%$, so $< 2\%$ is a conservative limit to stability. Other grid and strength parameters like non-local range rnl and center $centre$ are adapted from FRESCO's suggestions, while rnl is set to 0.5 fm larger than the largest rnl suggestion and $centre = 0$ is used. Few more step parameters are carefully adjusted and checked to ensure our work's credibility.

The post-form results together with experimental data [1] are presented in Fig. 2. In both energy scales, all three differential cross sections fit well with experiment in shape.

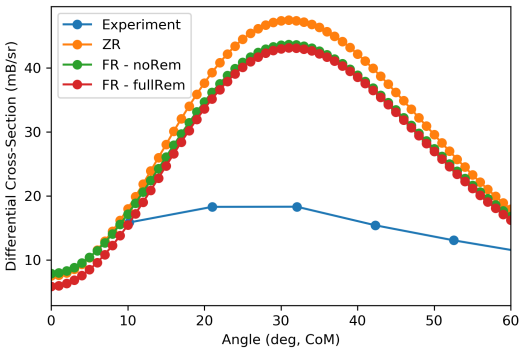

(a) 2.84 MeV experiment and post-form approximations.

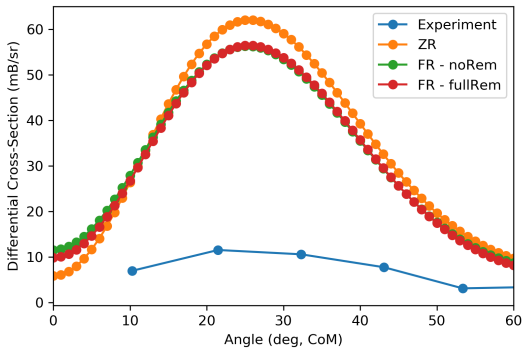

(b) 4.51 MeV experiment and post-form approximations.

Figure 2: Forward-angled differential cross sections calculated under: 1) zero-range approximation (ZR); 2) first-order DWBA finite range without remnant (FR - noRem); 3) first-order DWBA finite range with full complex remnant (FR - fullRem), as well as experimental data. Left and right panels are for 2.84 MeV and 4.51 MeV repectively.

Also, the agreement is better for 4.51 MeV case, as it gives more direct reactions than lower one. We can see that ZR approximation gives result deviates most from experiment because it applies the roughest approximation. It looks DWBA with or without remnants yield very similar results. This makes sense because U_{pA} and U_{pB} are so similar that they almost cancel each other in Eq. 3. But looking closer, we find the one with remnants is closer to experiment, which is for sure.

3 Results of prior-form DWBA calculations

In a transfer reaction A(d,p)B, the transfer T-matrix has a prior-form formula [4]

$$T_{prior} = \langle \Psi_2^{(-)}(\vec{r}_2, \vec{R}_2) \left| V_{nA}(r_n) + U_{pA}(r_p) - U_{dA}(R_1) \right| \phi_{np}\chi_{dA} \rangle, \tag{5}$$

where ϕ_{np} and χ_{dA} are bound states wave-functions, $\vec{r}_n = \vec{r}_p + \vec{r}_1$, and $U_{dA}(R_1)$ is the auxiliary potential we choose. Under first-order DWBA, it becomes

$$T_{prior}^{DWBA} = \langle \phi_{nA}\chi_{pB}^{(-)} \left| V_{nA}(r_n) + U_{pA}(r_p) - U_{dA}(R_1) \right| \phi_{np}\chi_{dA} \rangle, \tag{6}$$

The differential cross sections of ^{12}C(d, p)^{13}C calculated in both post and prior forms are given in Fig. ??. First-order DWBA with finite-range interactions and full complex remnant is used in both calculations. The convergence of calculation in prior form is checked in the same way as we discussed in Sec. 2. Variables *rnl* and *centre* are chosen based on FRESCO's recommendations. As shown in Fig. ??, the results from post- and

Table 1: Spectroscopic factors S extracted from ^{12}C(d, p)^{13}C. θ_p is the angle of the first peak, and σ^{exp} and σ^{DWBA} are corresponding differential cross sections obtained from experimental data and post-form DWBA calculation, respectively.

Beam energy (MeV)	2.84	4.51
θ_p (degree)	31	25
σ^{exp} (mb/sr)	18.49	11.57
σ^{DWBA} (mb/sr)	43.14	56.40
$S = \sigma^{\text{exp}}/\sigma^{\text{DWBA}}$	0.4286	0.2051

prior-form calculations have similar trends and are not far from each other. If we calculate without any approximation (Eq. 2 and 5), the same results should be obtained from both forms. But if only first-order DWBA is considered, we expect that small differences between the two results appear, which can be seen in Fig. ??.

It is worth mentioning that the recommended rnl, which represents the non-local range, is larger in prior form (??) than that in post form (??). In post form (Eq. 3) $U_{pA}(r_p)$ and $U_{pB}(R_2)$ are close to each other as nuclei A and B are very similar. Thus, the operator in Eq. 3 is approximately $V_{np}(r_1)$, which has a very short range. However, in prior form (Eq. 6) $U_{pA}(r_p)$ and $U_{dA}(R_1)$ cannot cancel each other as the elastic scatterings of deuteron on A and proton on A are very different. Thus, the operator in Eq. 6 has a longer range which comes from optical potentials $U_{pA}(r_p)$ and $U_{dA}(R_1)$. A larger rnl in prior-form calculation also leads to a longer runtime.

4 Extraction of spectroscopic factor

As is normal, the spectroscopic factor is extracted by comparing the theory to the data at the first peak in the angular distribution [5], as we expect that the reaction is mostly direct at the forward angle. The spectroscopic factors at beam energies 2.84 MeV and 4.51 MeV are given in Table 1. The angle of first peak θ_p is given by the calculations in Sec. 2, and σ^{exp} is obtained by spline interpolation of experimental data. The spectroscopic factors we extract are energy-dependent, which is expected because Ref. [1] shows that ^{12}C(d, p)^{13}C is more accurately modeled as a compound reaction at the beam energies we choose.

References

[1] T. W. Bonner, J. T. Eisinger, Alfred A. Kraus, and J. B. Marion. Cross section and angular distributions of the (d, p) and (d, n) reactions in c^{12} from 1.8 to 6.1 MeV. *Phys. Rev.*, 101:209–213, Jan 1956.

[2] Haixia An and Chonghai Cai. Global deuteron optical model potential for the energy range up to 183 MeV. *Phys. Rev. C*, 73:054605, May 2006.

[3] M.B.Chadwick and P.G.Young. Proton nuclear interactions up to 250 MeV for radiation transport sumulations of particle therapy. *Proc.Int. Particle Therapy Mtg. and PTCOG XXIV*, Apr 1996.

[4] Ian J Thompson and Filomena M Nunes. Nuclear reactions for astrophysics: principles, calculation and applications of low-energy reactions. pages 150–157, 2009.

[5] X. D. Liu, M. A. Famiano, W. G. Lynch, M. B. Tsang, and J. A. Tostevin. Systematic extraction of spectroscopic factors from $^{12}\mathrm{C}(d,p)^{13}\mathrm{C}$ and $^{13}\mathrm{C}(p,d)^{12}\mathrm{C}$ reactions. *Phys. Rev. C*, 69:064313, Jun 2004.